



INTERNATIONAL ATOMIC ENERGY AGENCY
UNITED NATIONS EDUCATIONAL, SCIENTIFIC AND CULTURAL ORGANIZATION
INTERNATIONAL CENTRE FOR THEORETICAL PHYSICS
I.C.T.P., P.O. BOX 586, 34100 TRIESTE, ITALY, CABLE: CENTRATOM TRIESTE



H4.SMR/782-21

**Second Workshop on
Three-Dimensional Modelling of Seismic Waves
Generation, Propagation and their Inversion**

7 - 18 November 1994

*Imaging of the Weathered Zone and
Estimation of Q in Sediments*

G. Costa - G.F. Panza - A. Vuan

Istituto di Geodesia e Geofisica
Università di Trieste
Trieste, Italy

**INTERNATIONAL CENTRE FOR
THEORETICAL PHYSICS**

**IMAGING OF THE WEATHERED ZONE
AND ESTIMATION OF Q IN SEDIMENTS**



**INTERNATIONAL
ATOMIC ENERGY
AGENCY**



**UNITED NATIONS
EDUCATIONAL,
SCIENTIFIC
AND CULTURAL
ORGANIZATION**

T. Mammo

A. Yuan

G. Costa

and

G.F. Panza

MIRAMARE-TRIESTE

International Atomic Energy Agency
and

United Nations Educational Scientific and Cultural Organization
INTERNATIONAL CENTRE FOR THEORETICAL PHYSICS

IMAGING OF THE WEATHERED ZONE
AND ESTIMATION OF Q IN SEDIMENTS

ABSTRACT

Phase - consistent filtering together with frequency time analysis (multiple filtering) is used to obtain the group velocity dispersion curve of the fundamental mode and first few higher modes of Rayleigh waves from seismic exploration data. The group velocities are then inverted to obtain shear wave velocity distribution to a depth of about 30 meters. The comparison of the experimental traces with the complete synthetic seismograms, computed using as input structural parameters of the inversion results, allow us to estimate the anelastic properties of the medium: Q (quality factor) values are observed to vary from 5 to 20.

T. Mammo

International Centre for Theoretical Physics, Trieste, Italy
and

Department of Geology and Geophysics, Science Faculty, Addis Ababa University,
Addis Ababa, Ethiopia.

A. Vuan, G. Costa

Istituto di Geodesia e Geofisica, Università degli Studi, Trieste, Italy

and

G.F. Panza

International Centre for Theoretical Physics, Trieste, Italy
and

Istituto di Geodesia e Geofisica, Università degli Studi, Trieste, Italy.

MIRAMARE - TRIESTE

November 1993

INTRODUCTION

In seismic exploration for hydrocarbons the source and the geophones are deployed on the surface of the earth in such a way to attenuate the undesired signals. One of these unwanted signals is represented by the fundamental mode and higher modes of Rayleigh waves and is termed in seismic literature as ground roll. The ground roll, that is not attenuated during the acquisition stage, obscures the reflected signals and makes them difficult to interpret. The seismic analyst consequently eliminates them by suitable processing techniques. However the ground roll in reality does contain information of the medium through which it propagates. In this paper we show how this information can be retrieved. The method commonly known as frequency - time analysis (FTAN) followed by phase - consistent filtering is employed to obtain the group velocity dispersion curve of the ground roll. Since the dispersion is primarily controlled by the shear wave velocity of the medium, the information retrieved from the data is inverted to obtain the S-wave velocity distribution versus depth.

Finally, by comparing experimental and synthetic seismic sections, constructed on the basis of the inversion of the dispersion data, it is possible to estimate the anelasticity of the medium.

In seismic exploration, the knowledge of the variation with depth of the S-wave velocity can be employed in what is termed as static correction, to enhance the quality of seismic data by improving the continuity of the reflected signals. Furthermore,

when the density is known, the shear modulus can be determined which, in combination with the quality factor Q , is important in studies of foundation vibrations, effects of earthquakes and slope stability (Gabriels, et al. 1987). Knowledge of the attenuation is important in the acquisition, processing and interpretation of high-resolution seismic data, vertical seismic profile data and borehole sonic log data as well as in the deduction of other physical properties such as permeability (Klimentos and McCann, 1990).

ANALYSIS OF RAYLEIGH WAVES

Diverse methods exist for the determination and analysis of Rayleigh modes. These methods utilize group velocities or phase velocities of fundamental mode and/or higher modes depending on the scope of the study. Gabriels et al. (1987) used the frequency-wavenumber domain to measure the dispersion properties of Rayleigh modes and obtained the phase velocity for the fundamental mode and the first 5 higher modes. Their method has an advantage in that it shows good resolution for higher modes. But the weakness of this method is that it requires the acquisition of a large amount of data and subsequently a large amount of computer time is needed in the processing stage (Jongmans, 1991). Moreover it suffers from aliasing whenever both the spatial and temporal samplings are not sufficiently small.

Another method used to calculate the phase velocity dispersion curve takes into consideration the entire wavefield

(McMechan and Yedlin, 1981). The method involves two linear transformations: slant stack and 1-D Fourier transform. Slant stack produces a wavefield in the phase slowness - time intercept (p-t) plane in which phase velocities are separated ($p=1/c$, c =phase velocity). The frequency associated with each phase velocity is then obtained by a 1-D Fourier transform over t . Thus the data wavefield is linearly transformed from the time-distance domain into the slowness - frequency ($p-\omega$) domain where dispersion curves are imaged. This method again suffers aliasing whenever sampling rates in both time and offset are not sufficiently high.

The method we employed to analyze the Rayleigh waves is FTAN (Levshin, et al 1972) which is quite an improved version of the multiple filter technique first introduced in digital form by Dziewonski et al. (1969). In this work we used FTAN followed by phase - consistent filtering (also called phase-matched filtering or phase equalization) to facilitate signal selection (Herrmann and Russell, 1990). Band pass filtering and windowing are also used where necessary. This method measures group velocity dispersion curve of a single seismic trace and as such doesn't employ much computer time and is free from the aliasing problem.

DATA ACQUISITION AND PROCESSING

The data were collected in North Africa in September 1987. The spread configurations for both the sources and the geophones are shown in fig.1. For each shot 120 receiver group arrays are employed. Sixty geophones are used in each group array.

Fifteen explosions, with a total weight of 18.75 kg, were fired simultaneously at a depth of 3 metres. Four seconds long time series having a sampling interval of 2 ms were collected. The frequency content of the data ranges from 4 Hz to 50 Hz. The figure number 2 shows an example of 60 traces acquired in the experiment. In this section the head waves, direct waves and ground roll are identified (fig. 3).

In fig. 4 three seismic traces extracted from the data are shown. In all these traces the ground roll can be observed. Indicating these Rayleigh modes with $X(t)$ we can compute the spectrum $S(\omega)$:

$$S(\omega) = \int X(t) \exp(-i\omega t) dt$$

We pass the spectrum through a system of narrow-band Gaussian filters $H(\omega)$ with varying central frequency ω_i .

$$H(\omega) = \exp\left(-\alpha\left(\frac{\omega - \omega_i}{\omega_i}\right)^2\right)$$

where α is the parameter controlling the resolving power of the filters.

The frequency-time representation of the output function is

$$Y(\omega, t) = \int S(\omega) \exp\left(-\alpha\left(\frac{\omega - \omega_i}{\omega_i}\right)^2\right) \exp(i\omega t) d\omega$$

The diagram $|Y(\omega, t)|$ is the signal envelope (ridge crest) and is useful for the determination of group velocities. On the diagram $\log|Y(\omega, t)|$ the dispersion curve $\tau(\omega)$ follows the ridge crest. The diagrams for the three traces after the application of deconvolution to remove the instrument responses, are shown in fig. 5. In all these diagrams one can see three zones of maximum amplitude concentrated around the velocity values of 230 m/s, 300-320 m/s and 450-470 m/s corresponding, respectively, to the fundamental mode and to the first few higher modes of Rayleigh waves. The similarity of the three diagrams indicates the absence of relevant lateral heterogeneity along the sampled path. Once the dispersion curve of each mode is approximately determined we can transform the signal into the non-dispersed one using phase-consistent filtering. The scope of this processing step is to remove arrivals not pertinent to the mode under consideration, that we call here noise. The procedure is as follows. On the diagram $\log|Y(\omega, t)|$ approximate group time $\tilde{\tau}(\omega)$ values are identified at some discrete frequencies and subsequent cubic spline interpolation performed.

Approximate phase delay $(\tilde{\phi}(\omega))$ of the signal is then calculated from the group time (Ratinkova, 1990; Shapiro, 1992).

$$\tilde{\phi}(\omega) = - \int_0^\omega \tilde{\tau}(\eta) d\eta + C_1 \omega + C_2$$

where C_1 and C_2 are constants.

Now we add

$$- \int_0^\omega \tilde{\tau}(\eta) d\eta - C_1 \omega - C_2$$

to the true phase spectrum $\phi(\omega)$ of the signal. If the phase spectrum $(\tilde{\phi}(\omega))$ is a reasonable approximation to the true phase spectrum $\phi(\omega)$ then $|\phi(\omega) - \tilde{\phi}(\omega)|$ is sufficiently close to zero and the inverse transformation will give a compressed or undispersed signal shifted to a certain instant of time, which is controlled by the constants C_1 and C_2 . The noise will be either spread out or, if compressed, is compressed slightly and located away from the signal. The noise is then removed with the application of an amplitude time window to obtain a filtered signal which is subsequently transformed into the frequency domain. The final step is to restore the original phase by adding

$$- \int_0^\omega \tilde{\tau}(\eta) d\eta + C_1 \omega + C_2$$

to the phase spectrum $\phi(\omega)$. The output of this final step is seen in fig.6.

INVERSION FOR GROUP VELOCITY AND Q

In fig.6 one can see that FTAN analysis permits the separation of various modes. The fundamental mode is shown in (a). The higher modes in (b) and (c). The higher modes, are interpreted as first and third respectively by comparing their dispersion curves with the synthetic ones, computed for a structural model

consistent with the fundamental mode dispersion. Due to the structural properties, in the frequency band considered, the second higher mode is not excited, and the modes of higher number cannot be well separated due to their very similar group velocities. Therefore we have decided to invert the dispersion curves of the fundamental and the first higher mode keeping the dispersion curve of the third higher mode only for a qualitative control of the inversion results. Once the modes are identified the next step is to perform their inversion. The dispersion curves of Rayleigh modes are primarily sensitive to the shear wave velocity and therefore they can be inverted in order to find the S-wave velocity distribution with depth. The inversion is undertaken by the hedgehog method, developed by Keilis-Borok and Yanovskaja (1967), and discussed in detail by Panza (1981).

In this procedure an initial structural model is considered. This model is represented by a set of parameters whose values vary with depth. We constructed the model from the analysis of the first arrivals and sonic and density logs. Perturbing the part of the initial model which is mostly sensitive to the available data, group velocities corresponding to all periods determined in the data processing are computed. These velocities are then compared with the observed velocities of equal periods. If the difference between the computed and the observed values for any of the periods exceeds the pre-set threshold value the model is rejected and another model in the neighbourhood of the first is considered, and the procedure repeated. If, on the other hand, the difference is below the pre-set limit for the longest period the procedure extends to the next shorter period. If the difference is below the threshold limit for all periods the model is accepted provided that

the r.m.s., σ , of the entire data set is less than the pre-set threshold. In our case all models with $\sigma \leq 8$ m/s are accepted. The error of each frequency point has been estimated on the basis of repetition of dispersion measurements for more traces and is given in tab. 1.

Frequency(hz)	Error(m/s)
7.09	10
8.92	8
11.11	7
13.69	6
16.66	5
8.13	25
8.47	20
9.34	18
11.11	15
16.66	12
19.23	9

Tab. 1 - Frequency values with observation error used in the inversion. The first five values belong to the fundamental mode while the next six to the first higher mode.

The different solutions of the inverse problem are contained within the stripe defined by the dashed lines that are shown in fig. 7; in the same figure the solid line represents the starting model used in computations. Values of the V_p/V_s ratio versus V_s obtained from the inversion are given as solid little balls in figure 8; as it can see from the figure these values are in quite good agreement with the measurements, made by Stumpel et al. (1984), for dry and partially saturated sands.

The availability of the distribution versus depth of the elastic parameters and of the density allows us to compute

complete synthetic seismograms (Panza, 1985) and therefore to determine the anelastic properties of the medium (Craglietto et al., 1989). Since local site effects, scattering and lateral lithological changes prevent meaningful direct measurement of amplitude decay (Mokhtar, et al. 1988), quality factor (Q) values can be estimated by direct comparison of experimental and synthetic data (Craglietto et al., 1989). Initially very high and very low values of Q are selected. Subsequently the range between these extreme values is narrowed until we get a satisfactory matching between the synthetic and experimental data, special attention being paid to the similarity of signal envelopes. An example of synthetic data, to be compared with the experimental ones shown in fig. 2, is given in fig. 9. Similar signals are obtained using, in the computations, Q values which are variable in the ranges given in table 2:

Depth (m)	Quality factor
0 - 31	5 - 20
31 - 490	25 - 60
490 - 2200	25 - 120

Tab. 2. Derived distribution versus depth of Q values.

CONCLUSION

From seismic reflection data it is possible to retrieve the S-wave velocity distribution versus depth from the dispersion curve of Rayleigh modes, determined using frequency-time analysis and phase-consistent filtering. The method used doesn't suffer from aliasing and doesn't require large amounts of computer time since

data from single stations are used. The result obtained, about the elastic properties, is comparable to that described by Gabriels et al. 1987, who used the stacking of 256 stations. Here, in addition, with the use of complete synthetic seismograms, we have given an estimate quality of the quality factor, Q.

ACKNOWLEDGEMENTS

This research was performed during the visit of one of us (M. Tilahun) at the Istituto di Geodesia e Geofisica of Università degli Studi di Trieste, as Associate of the International Centre for Theoretical Physics.

The study has been made possible by the financial support from CNR (contract 92.02867.54) and MURST (40% and 60% funds).

We would like to acknowledge very useful discussions with Dr. A. Mazzotti.

REFERENCES

- CRAGLIETTO, A., PANZA, G.F., MITCHELL, B. J. and COSTA, G., 1989, Anelastic properties of the crust in the Mediterranean area, American Geophysical Union, Geophysical Monograph 51, IUGG, 6, 179 - 196.
- DZIEWONSKI, A., BLOCH, S. and LANDISMAN, M. 1969, A technique for the analysis of transient seismic signals, *Bull. Seism. Soc. Am.*, 59, 427-444.
- GABRIELS, P., SNIEDER, R. and NOLET, G. 1987, In situ measurements of shear-wave velocity in sediments with higher-mode Rayleigh waves, *Geophysical Prospecting*, 35, 187-186.
- HERRMANN, R. and RUSSELL, D. 1990, Ground roll: Rejection using adaptive phase-matched filters, *Geophysics*, 55, 776-781.
- JONGMANS, D. 1991, L'influence des structures géologiques sur l'amplification des ondes sismiques. *These de Docteur en Sciences Appliquées*, Université de Liège.
- KEILIS-BOROK, V. and YANOVSKAJA, T. 1967, Inverse problems of seismology (structural review), *Geophys. J. R. Astr. Soc.*, 13, 223-234.
- KLIMENTOS, T. and McCANN, C. 1990, Relationships among compressional wave attenuation, porosity, clay content, and permeability in sandstones, *Geophysics*, 55, 998-1014.
- LEVSHIN, A., PISARENKO, V. and POGREBINSKY, G. 1972, On a frequency-time analysis of oscillations, *Annales Geophys.*, 28, 211-218.
- McMECHAN G. and YEDLIN, M. 1981, Analysis of dispersive waves by wavefield transformation, *Geophysics*, 46, 869-874.
- MOKHTAR, T., HERRMANN, R. and RUSSELL, D. 1988, Seismic velocity and Q model for shallow structure of the Arabian shield from short period Rayleigh waves, *Geophysics*, 53, 1379-1387.
- PANZA, G. 1981, The resolving power of seismic surface wave with respect to crust and upper mantle structural models, in *The solution of the inverse problem in Geophysical Interpretation*, R. Cassinis (ed.), 39-77, Plenum press.
- PANZA, G. 1985, Synthetic seismograms: the Rayleigh waves modal summation, *J. Geophys.*, 58, 125-145.
- RATINKOVA, L. 1990, Frequency-time analysis of surface waves, Workshop on "Earthquake Sources and Regional Lithospheric Structures From seismic Wave Data", Nov.19-30, 1990, I.C.T.P., Trieste.
- SHAPIRO, N. 1992, Frequency-time analysis of surface waves, Workshop on Three - Dimensional Modelling of Seismic Waves Generation, Propagation and their Inversion, Nov.30 - Dec.11, 1992, I.C.T.P., Trieste.
- STUMPEL H., KHALER S., MEISSNER R. and MILKEREIT B., 1984, The use of seismic shear waves and compressional waves for lithological problems of shallow sediments, *Geophysical Prospecting*, 32, 662-675.

FIGURE CAPTIONS

- Figure 1 - Spread configuration, a) source and b) geophone patterns.
- Figure 2 - Example of available data sets (channels 61 to 120 from shot n.1).
- Figure 3 - Schematic representation of main phases visible in the section: H) head wave, D) direct wave, G) ground roll.
- Figure 4 - Example of signals that have been processed:
a) trace n.68 with source - geophone distance equal to 630 m.; b) trace n.71 (distance 750 m.);
c) trace n.72 (distance 810 m.).
- Figure 5 - Frequency time analysis diagram for the traces shown in fig. 4. To darker areas correspond larger amplitudes
- Figure 6 - Example of the dispersion curves obtained; a) fundamental mode, b) first higher mode and c) third higher mode.
- Figure 7 - Schematic representation of the solution of the inverse problem; the solid line represents the model used in calculations and dashed lines contain the number of possible models.
- Figure 8 - V_p/V_s ratio versus V_s for sands (dry and partially saturated) (from Stumpel et al., 1984) in relation with our results

Figure 9 - Synthetic section computed using a single point instantaneous explosive source and a single geophone for channel.

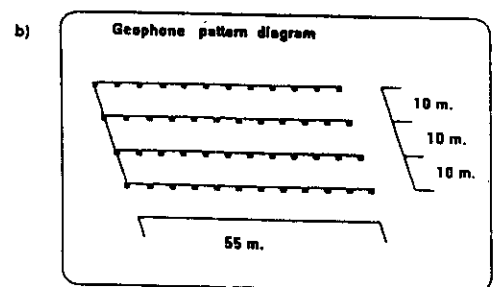
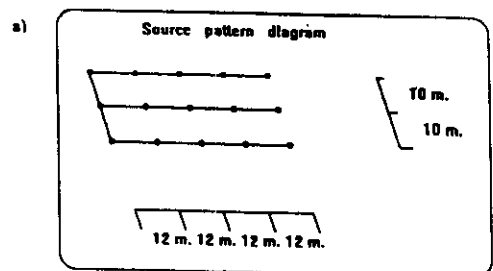
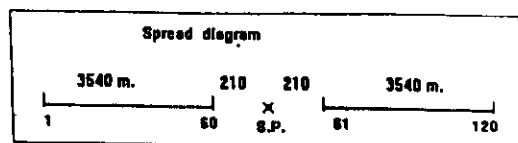


Fig. 1

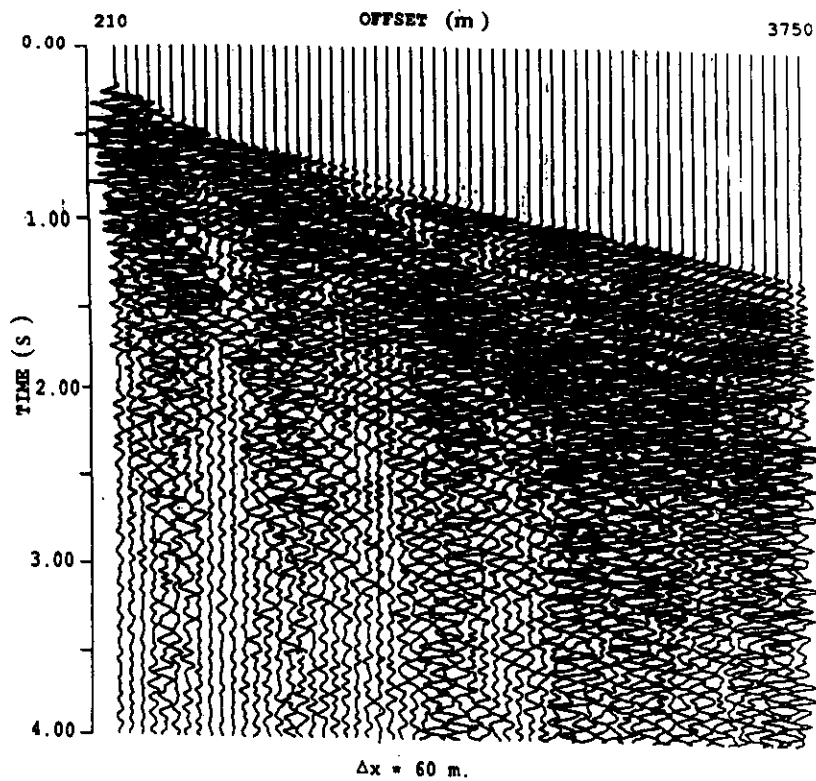


Fig. 2

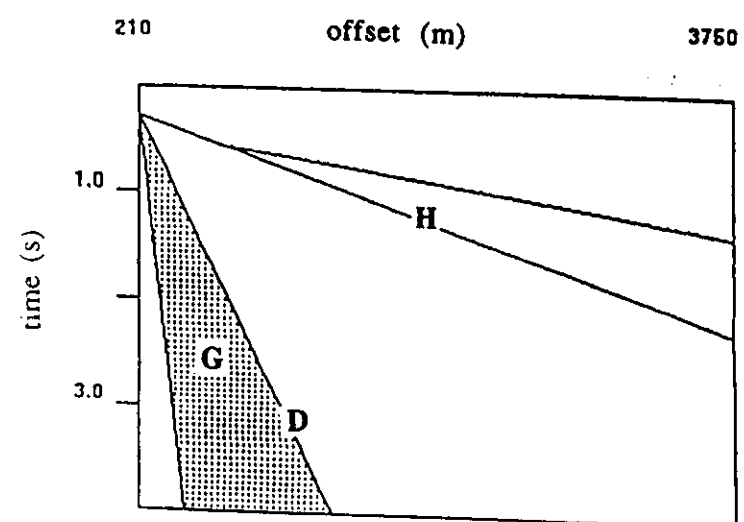


Fig. 3

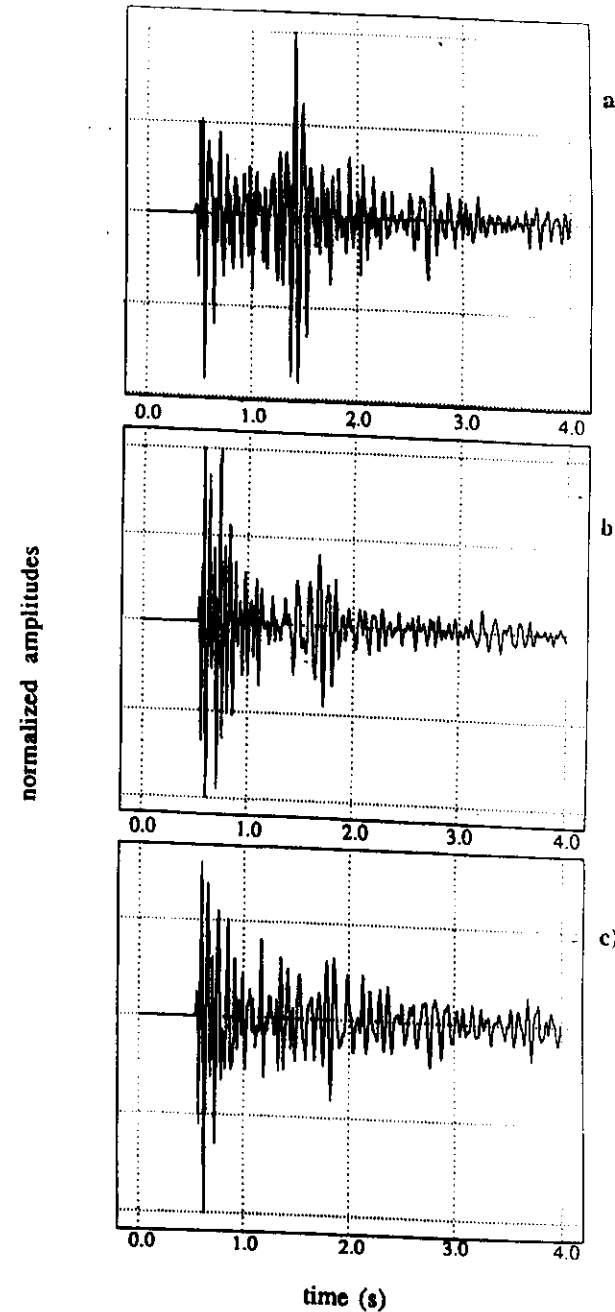


Fig. 4

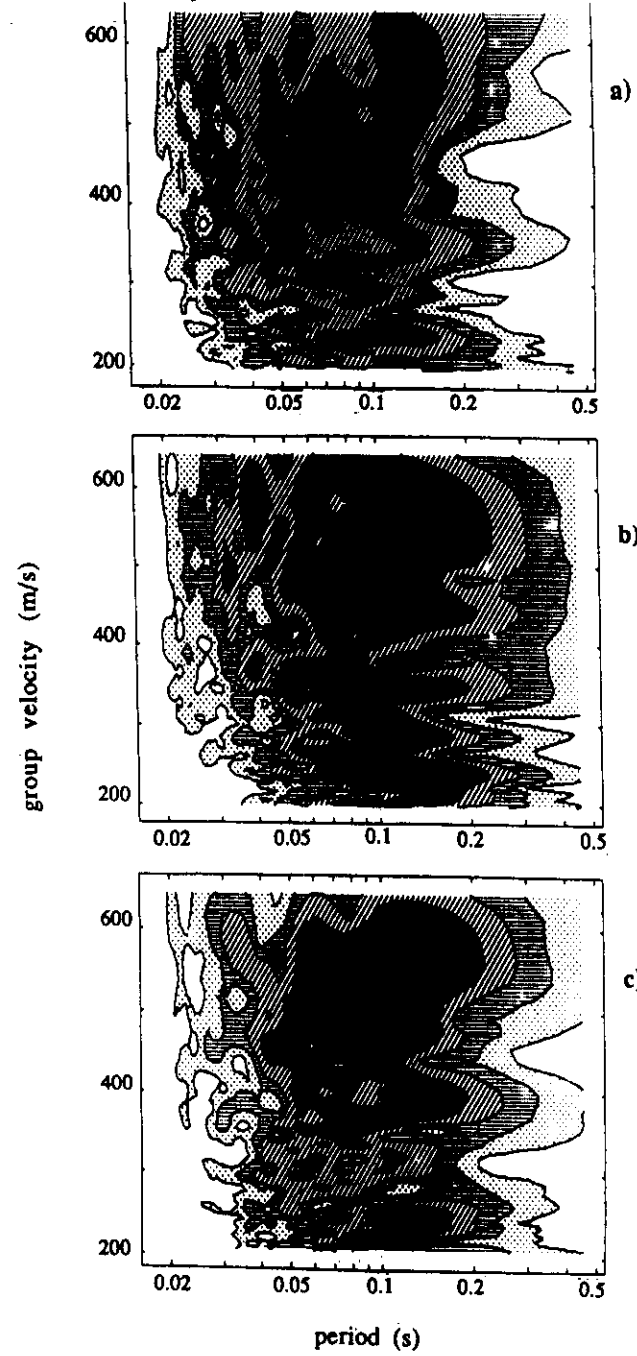


Fig.5

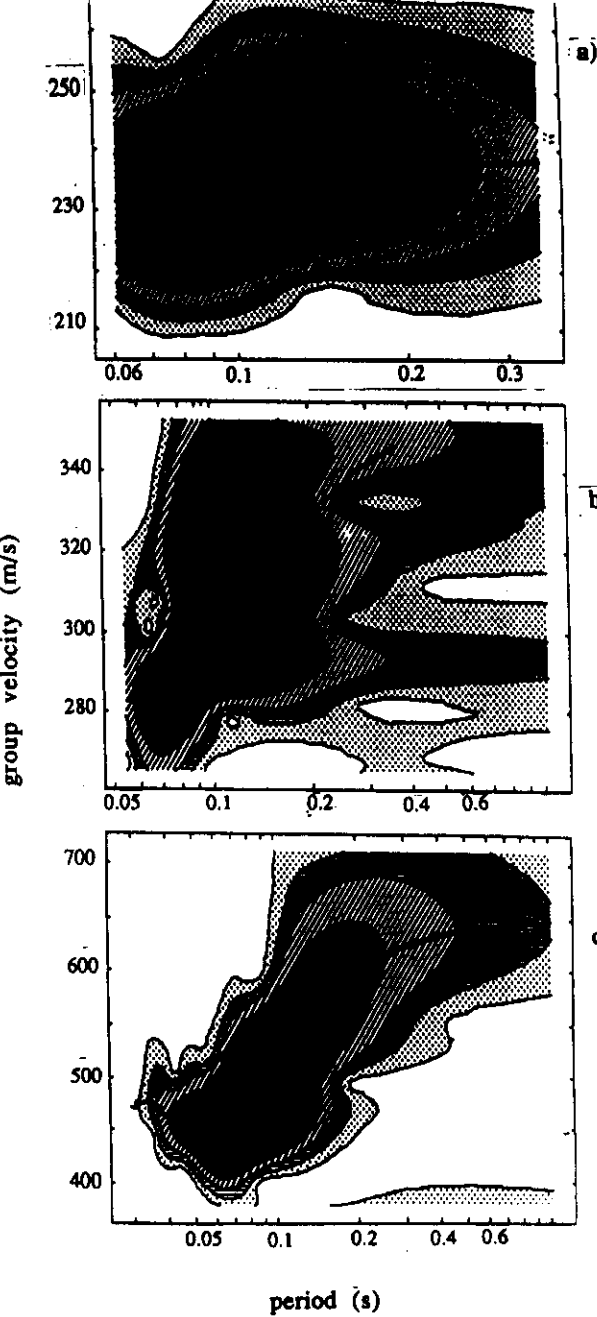


Fig.6

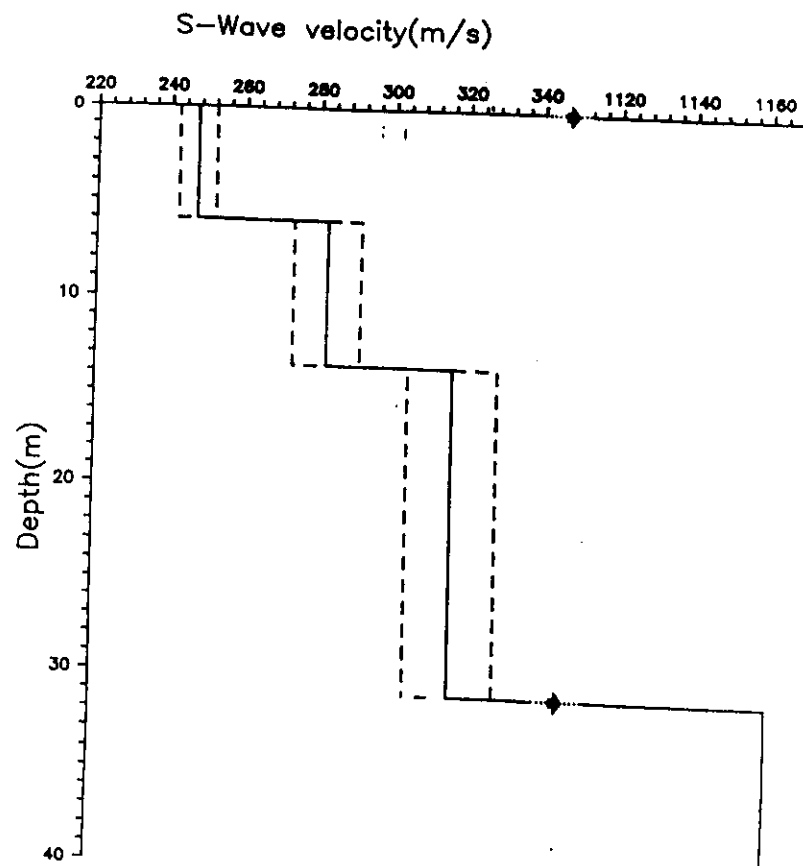


Fig.7

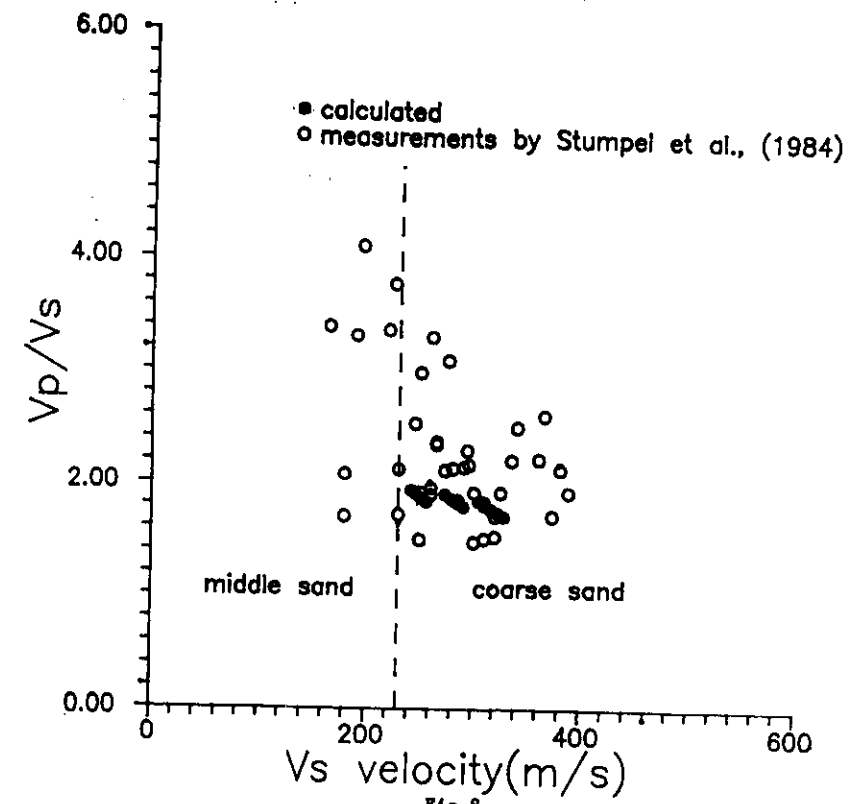


Fig.8

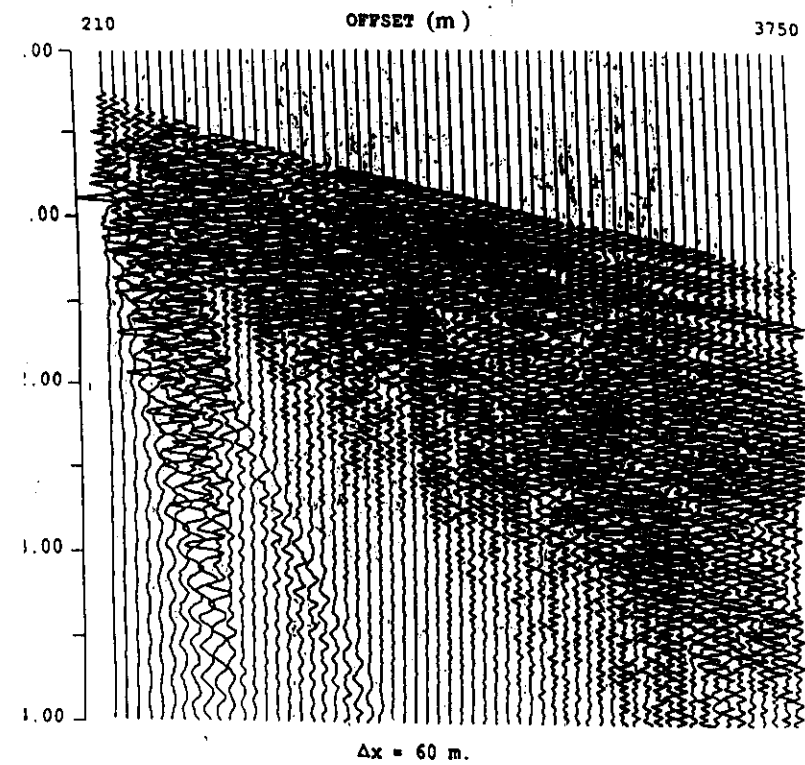


Fig. 9

